

## Hot-electron relaxation in quartz using high-order harmonics

F. Quéré, S. Guizard, Ph. Martin, and G. Petite

*Service de Recherche sur les Surfaces et l'Irradiation de la Matière, DSM-DRECAM CEA Saclay, 91191 Gif-sur-Yvette, France*

H. Merdji, B. Carré, J-F. Hergott, and L. Le Déroff

*Service de Recherche sur les Photons, Les Atomes et les Molécules, DSM-DRECAM CEA Saclay, 91191 Gif-sur-Yvette, France*

(Received 21 January 2000)

Using ultrafast time-resolved ultraviolet photoelectron spectroscopy, we have followed the energy relaxation kinetics of conduction electrons in quartz, for energies of the order of 30 eV above the conduction-band minimum. We measure energy-loss rates three orders of magnitude lower than those estimated for energies close to this minimum. Likewise, the impact ionization rate obtained ( $1/40 \text{ ps}^{-1}$ ) is much lower than the values generally assumed in optical breakdown models.

The effects of a high level of electronic excitation in a dielectric depend to a large extent on the conduction electron relaxation dynamics. This matter is central to a large variety of interactions between radiation and matter, such as, e.g., the effect of swift heavy ions in wide-band-gap dielectrics (controversy between “thermal spike” and “Coulomb explosion” models), the breakdown of dielectric materials under high dc fields, or the optical breakdown under strong laser fields. In these last two problems, the energy of carriers is ruled by the competition between the gain due to acceleration in the dc field or to the absorption of photons (free-carrier heating), and the losses due to electron-phonon collisions (leading to lattice heating). Depending on this competition, some electrons might gain enough energy from the field to collide with valence-band electrons (impact ionization), which might result in an electronic avalanche (an exponential growth of the number of excited electrons). The debate on the conditions in which such an avalanche can occur and be responsible for the breakdown of dielectrics has been open for more than 20 years,<sup>1-3</sup> and has been revived by recent ultrashort laser studies.<sup>4</sup> Because of its crucial importance both in optics and electronics, an impressive literature has been published concerning these problems in quartz. By directly measuring the relaxation of hot electrons in the conduction band of this material, in addition to providing some knowledge on this prototype for ionocovalent wide-band-gap insulators, we would like to clarify this debate.

To access ultrafast relaxation processes, the most suitable tool is subpicosecond lasers, especially two-color time-resolved photoemission spectroscopy:<sup>5,6</sup> a first pulse (pump) excites electrons in the conduction band, whereas a second pulse (probe) reexcites and ejects part of them out of the solid where their kinetic energy is measured. By varying the pump-probe delay, one gains access into the temporal evolution of the energy distribution. High-order harmonics generation in rare gases is a convenient way to extend these experiments into the vacuum ultraviolet (VUV) range, since it provides pulses that are synchronous with and as short as the laser pulses that generate them.<sup>7</sup> Such time-resolved ultraviolet photoelectron spectroscopy (TR-UPS) has already been performed to study electron dynamics at semiconductor surfaces,<sup>6</sup> the harmonics being used as a probe in these experiments.

In this paper we present an experiment aimed at a direct measurement of the relaxation of excited electrons in  $\alpha$ -SiO<sub>2</sub>, where we use the 25th harmonic ( $H_{25}$ ) of a Ti-Sa laser (38.7-eV photons) as a *pump*. The Ti-Sa laser delivers 60-fs pulses at 800 nm with energies up to 100 mJ, at a repetition rate of 20 Hz. 20 mJ are used to produce high-order harmonics of the laser, by focusing in an argon gas jet, as described in Ref. 8. The 25th harmonic is selected by a combination of a thin (100 nm) aluminum foil and of a 3-m focal length boron-silicon mirror at near normal incidence, which focuses the VUV beam onto the sample. This reflective setup allows us to preserve the pulse duration (60 fs) that a grating would have considerably increased. Another part of the laser beam is used to generate the probe beam at 800 or 400 nm (1.55 or 3.1 eV). It is focused onto the sample with a 3-m lens, at a 60° incidence. The interaction region on the sample is imaged with a camera to measure the probe beam size, as well as to control the time and space superposition: by removing the aluminum foil, interferences between the two beams at 800 nm are easily observed at a zero time delay. The probe pulse size and energy are typically 200  $\mu\text{m}$  and 100  $\mu\text{J}$ , leading to an intensity of a few  $\text{TW}/\text{cm}^2$ . Photoelectrons are detected using an eight-channel spherical electron energy analyzer with a resolution of 100 meV. Considering the spectral width of  $H_{25}$  (250 meV), and of the probe at 800 nm (40 meV), this gives an overall energy resolution of the order of 300 meV.

The 1-mm-thick quartz samples are cleaned in a dilute fluoridric acid solution (5%), and heated during 12 h at 1200 K in open air to preserve the surface stoichiometry. The ultrahigh-vacuum chamber ( $10^{-10}$  mbar) is equipped with a helium discharge lamp (He II), and the absence of any pollution can be checked by recording the UPS spectrum. The agreement between the spectra obtained with He II and  $H_{25}$  is quite good: the three well-known structures of the valence band of  $\alpha$  quartz<sup>9</sup> are easily recognizable, indicating that the surface is clean under operational conditions (Fig. 1). We do not know the origin of the differences in the low-energy peak amplitudes, but the high-energy edge (between 30 and 38 eV) that will be studied in detail in this paper is particularly well reproduced. Two important points, specific to photoemission experiments on insulators, must be underlined: (i)

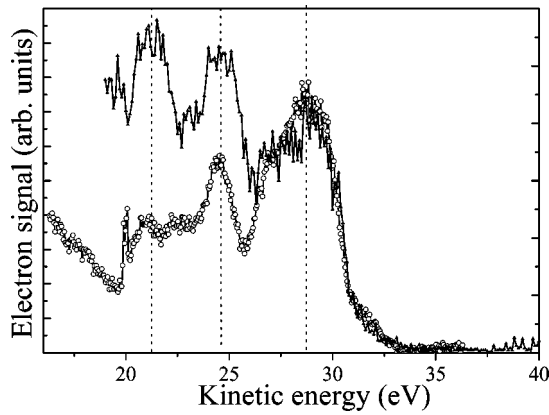


FIG. 1. UPS spectra of quartz obtained with the He II line (40.8 eV, circles), and with  $H25$  (38.75 eV, triangles). The former has been shifted to lower energies to allow a direct comparison.

to obtain a stable and reproducible signal, whatever the light source used, it is necessary to heat the quartz sample at 700 K in order to cancel artifacts due to charge buildup at the sample surface during the irradiation, and (ii) it is necessary to decrease the number of photons in each harmonic pulse down to a few  $10^6$  to avoid space-charge distortion of the UPS spectrum. We estimate the density of carriers excited by the pump to be of the order of  $10^{15} \text{ cm}^{-3}$ . Under such conditions, we are free of space-charge effects.

Let us see now what happens when the probe beam is added. In Fig. 2 we present the high-energy edge of the spectrum obtained with  $H25$  alone, and for two different delays between pump ( $H25$ ) and probe (IR, 1.55-eV photon). When the delay is set to zero, the spectrum is shifted toward high energies by approximately one IR photon energy. For positive delays (IR arrives *after*  $H25$ ) this shift decreases, and finally vanishes for delays larger than about 50 ps. Clearly these spectra suggest that electrons absorb one pump and then one probe photon, and that some relaxation occurs when the pump/probe delay increases. In contrast, for negative delays (IR arrives *before*  $H25$ ) spectra keep the same shape

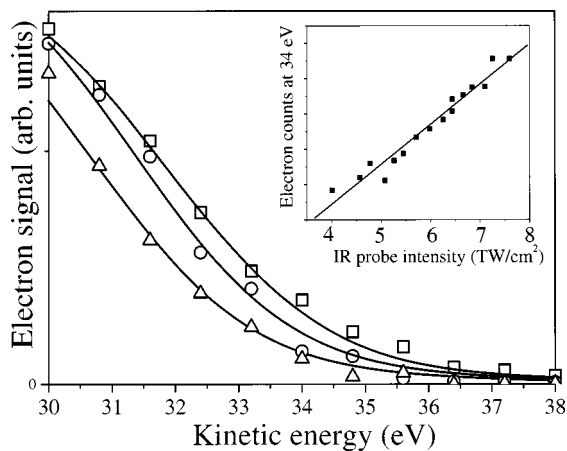


FIG. 2. High-energy edge of the UPS spectrum without probe (triangles), and when the UV pump pulse is followed by an IR probe pulse. Delay 0: squares. Delay 12 ps: circles. Simulations: solid lines. Inset: electron signal as a function of the IR probe intensity at a fixed energy (34 eV), a fixed harmonic intensity, and zero delay. The solid line is a guide for the eye.

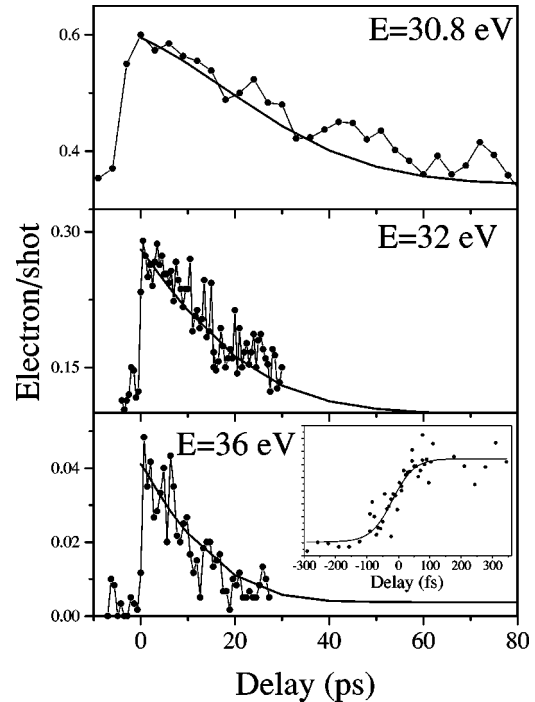


FIG. 3. Electron signal as a function of pump-probe delay for three energies in the high-energy part of the UPS spectrum. Solid lines: simulations. Inset: pump plus probe photoemission signal for short delays, at  $E = 36$  eV. The solid line is a guide for the eye.

and position as the one corresponding to  $H25$  alone. This reproducible behavior can be deeply modified when the pump and/or probe intensities are too large, indicating the presence of space-charge effects.

To obtain more precise information, we recorded the photoelectron signal at a fixed energy, as a function of the delay. Results at different kinetic energies in the high-energy tail of the spectrum (30.8, 32, and 36 eV) are shown in Fig. 3 for a probe at 800 nm. For each of these energies, we observe a strong increase of the signal at zero delay. For small negative delays, the kinetics correspond for all energies to the cross-correlation of both pulses (100 fs; see the inset of Fig. 3), whereas for positive delays we observe a slow decrease of the signal that is faster for higher kinetic energies. The simplest interpretation of these data would be an energy-dependent depopulation rate  $A_E$ , due, for instance, to impact ionization. This hypothesis implies an exponential decay of the signal which poorly fits the experimental curves, and gives values of  $A_E$  of the order of  $0.1 \text{ ps}^{-1}$  for 36-eV electrons and  $0.02 \text{ ps}^{-1}$  for 30-eV electrons. Clearly, such a strong variation in this small energy window far from the threshold is unlikely. Thus we interpret our results as follows: the decrease of the signal is due to the ejection of the electrons out of the solid, or to inelastic processes like impact ionization, which induce energy losses larger than the experimental window that we consider (i.e., around 10 eV). These different processes cannot be distinguished experimentally, and we assume that they occur at a rate  $A$  which varies negligibly in our energy window. In addition, some excited electrons remain in the conduction band for a time long enough to lose part of their energy before escaping into the vacuum. This means that at delay  $\tau$  we detect electrons that have lost some energy  $\Delta E$  between the absorption of a

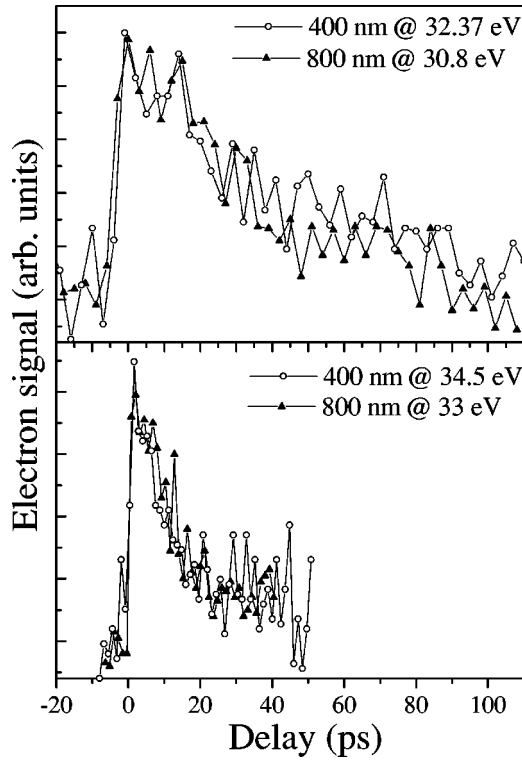


FIG. 4. Kinetics measured with an 800-nm probe at energy  $E$  (triangles), and with a 400-nm probe at energy  $E + \hbar\omega$  (circles), for  $E = 30.8$  and  $33$  eV.

pump and a probe photon. This explains the slowest kinetics at  $30.8$  eV, since the energy possibly lost by the electrons before absorbing a probe photon—and thus the time elapsed before doing so—is the largest in this case. Thus these measurements give a direct access to the relaxation dynamics of electrons in the conduction band. To validate this interpretation, we performed the same measurements using the second harmonic as a probe. We expect to observe the same kinetics when the detector energy is set at  $E$  for a probe at  $800$  nm, and at  $E + \hbar\omega$  ( $\hbar\omega$  is the energy of an  $800$ -nm photon) for a probe at  $400$  nm, since in both cases we measure the relaxation of electrons having an energy  $E - \hbar\omega$ . The results obtained for the two different probe wavelengths are in remarkable agreement in both cases, as shown in Fig. 4.

To interpret our results more quantitatively, we made a simulation based on a master equation:

$$\frac{df(E,t)}{dt} = Wf(E + \Delta E, t) - (W + A)f(E, t).$$

$f(E, t)$  is the probability for the state of energy  $E$  to be occupied at a time  $t$ .  $W$  is the probability per unit time that an electron jumps from  $E$  to  $E - \Delta E$ , and  $A$  represents all the population loss terms. The photoelectron spectrum obtained with the pump pulse only is proportional to the following quantity:  $S(E) = \int_0^\infty f(E, t) dt$ .

The probe pulse shifts a fraction of the distribution  $f(E, t)$  by  $\hbar\omega$  with an efficiency equal to the probability to absorb one photon ( $\alpha_+$ ), and by  $-\hbar\omega$  for the emission ( $\alpha_-$ ). For a given delay  $\tau$ , between the  $H25$  and the IR, the recorded spectrum will be

$$S(E, \tau) = \int_0^\tau f(E, t) dt + (1 - \alpha_+ - \alpha_-) \int_\tau^\infty f(E, t) dt \\ + \alpha_+ \int_\tau^\infty f(E - \hbar\omega, t) dt + \alpha_- \int_\tau^\infty f(E + \hbar\omega, t) dt.$$

To reproduce our results, we found that the absorption coefficient ( $\alpha_+$ ) must be larger than the emission coefficient ( $\alpha_-$ ) by roughly one order of magnitude, and for the sake of simplicity we have neglected it. The best fit of the spectra in Fig. 2 is obtained with  $\alpha_+ = 0.7$ , which means that 70% of the excited electrons have absorbed one probe photon. Non-linear effects like multiple-photon absorption are also expected. However, the signal was observed to increase linearly with the probe intensity (see the inset in Fig. 2), and multiphoton processes have therefore been neglected in the simulation. The fitting procedure consists of determining the initial energy distribution  $f(E, t=0)$  and the parameters  $W$  and  $A$  that give the best agreement with both the experimental time-dependent spectra and the relaxation kinetics for different energies (Figs. 2 and 3). For the energy relaxation rate  $W$  and the population loss rate  $A$ , we find  $70$  meV/ps and  $1/40$  ps $^{-1}$ , respectively.

As already mentioned, the rate  $A$  represents all processes that induce a population loss in the experimental energy window, and therefore gives an *upper value* for the impact ionization probability. A formula giving the collision rate between valence and conduction electrons in semiconductors was derived by Keldysh:<sup>10</sup>  $A = \tau_0 [(E - E_G)/E_G]^2 s^{-1}$ , which assumes that the kinetic energy ( $E$ ) is close to the ionization threshold ( $E_G$ ), and that the band structure is spherical and parabolic. A crude estimation using this formula gives an impact ionization rate of  $6$  fs $^{-1}$ ,<sup>11</sup> i.e., more than five orders of magnitude larger than what we measure. However, such a discrepancy is not so surprising, since the prefactor  $\tau_0$ , which is proportional to the product of the two overlap integrals between the initial and final states for each electron, is completely unknown in the case of  $\alpha$ -SiO $_2$ . Indeed as pointed out in Ref. 12 in the case of GaAs, different approaches to evaluate this prefactor give results that differ by a factor 300. Clearly a more sophisticated description of the band structure is needed to clear up this point. Experimentally, only one investigation aiming at the measure of impact ionization rate was published<sup>14</sup> in the case of a SiO $_2$ /Si overlayer, giving an impact ionization rate of  $3$  fs $^{-1}$  for 16-eV electrons. Because the density of defects in oxide films from  $5$  to  $20$  Å may be orders of magnitude higher than in our pure quartz monocrystal or larger thickness samples, a direct comparison may be questionable. Indeed, these authors also pointed out that for larger oxide thicknesses ( $50$ – $100$  nm) such high relaxation rates were unable to fit their results.<sup>1</sup>

The measured relaxation rate ( $W$ ), which is essentially due to the coupling with optical phonons, is quite small if compared to numerical simulations.<sup>13</sup> Indeed, according to a semiclassical theory based on the Boltzmann equation, calculations using the Fröhlich Hamiltonian<sup>15</sup> predict an energy-loss rate of  $20$  eV/ps for 2-eV electrons (unfortunately no *direct* experiments have been performed in this “low” energy region) and  $5$  eV/ps for 30-eV electrons. This last rate is 70 times larger than what we measure. It is not

clear at this stage if the assumptions of this model (isotropic and parabolic band structures) could explain such a quantitative discrepancy; however, more fundamentally, all these simulations, because based on the Fermi golden rule, suppose that energy is strictly conserved between successive collisions. If the scattering rates are larger than the time necessary to exchange an optical phonon ( $1/\omega_{lo} \sim 40$  fs for 100-meV phonons), then semiclassical descriptions are no longer valid. Because we are using this case (5 eV/ps corresponds to a scattering rate of 20 fs for 100 meV), quantum calculations are absolutely necessary to take into account the non-Markovian behavior of the system. This problem was pointed out by several authors, and the results published so far<sup>17,18</sup> indicated, indeed, longer *effective* energy relaxation times than those predicted by semiclassical calculations. However, if the agreement between our measurements and the semiclassical theory is not *quantitatively* good, let us note that the absorption probability  $\alpha_{+} = 0.7$  corresponds to an absorption cross section of  $8 \times 10^{-19}$  cm<sup>2</sup>, more than one order of magnitude smaller than the one we measured

( $10^{-17}$  cm<sup>2</sup>) at lower electron kinetic energies,<sup>16</sup> which is consistent with a decrease of the electron-phonon scattering rate as predicted by all theories.

We have demonstrated an unexpectedly long “lifetime” for electrons with energies 30 eV above the bottom of the conduction band in quartz. A simulation of our results, based on a kinetic model, gives a relaxation rate of 70 meV/ps. We also found an upper value for the impact ionization rate of  $1/40$  ps<sup>-1</sup>. Thus ionizing collisions with valence-band electrons do not appear as a very efficient relaxation mechanism, and this result should be taken into account, for instance, in the interpretation of recent experiments concerning laser-induced breakdown. This work shows that TR-UPS is a powerful tool to explore relaxation processes in all kinds of solids, and should provide valuable information and stimulate theoretical approaches.

We gratefully acknowledge P. Salières, M. J. Guittet, M. Henriot, M. Bougeard, O. Gobert, P. Meynadier, and M. Perdrix for advice and stimulating discussions.

<sup>1</sup>E. Cartier *et al.*, Rev. Solid State Sci. **5**, 531 (1991).

<sup>2</sup>S. C. Jones *et al.*, Opt. Eng. (Bellingham) **28**, 1039 (1989).

<sup>3</sup>N. Bloembergen, IEEE J. Quantum Electron. **QE-10**, 375 (1974).

<sup>4</sup>Ming Li *et al.*, Phys. Rev. Lett. **82**, 2394 (1999); M. Lenzner *et al.*, *ibid.* **80**, 4076 (1998); B. C. Stuart *et al.*, *ibid.* **75**, 2248 (1995).

<sup>5</sup>R. T. Williams *et al.*, Opt. Eng. (Bellingham) **28**, 1085 (1989).

<sup>6</sup>R. Haight, Surf. Sci. Rep. **21**, 275 (1995).

<sup>7</sup>A. L’Huillier *et al.*, in *Atoms in Intense Laser Fields*, edited by M. Gavrilá (Academic Press, San Diego, 1992).

<sup>8</sup>Ph. Martin *et al.*, Laser Phys. **10**, 1 (2000).

<sup>9</sup>F. Jollet and C. Noguera, Phys. Status Solidi B **179**, 473 (1993).

<sup>10</sup>L. V. Keldysh, Sov. Phys. JETP **37**, 509 (1960).

<sup>11</sup>B. C. Stuart *et al.*, Phys. Rev. B **53**, 1749 (1996).

<sup>12</sup>B. K. Ridley, *Quantum Processes in Semiconductors* (Clarendon Press, Oxford, 1993).

<sup>13</sup>M. V. Fischetti *et al.*, Phys. Rev. B **31**, 8124 (1985).

<sup>14</sup>E. Cartier *et al.*, Phys. Rev. B **44**, 10 689 (1991).

<sup>15</sup>H. Fröhlich, Proc. R. Soc. London, Ser. A **160**, 230 (1937).

<sup>16</sup>Ph. Daguzan *et al.*, J. Opt. Soc. Am. B **13**, 138 (1996).

<sup>17</sup>Ph. Daguzan *et al.*, Phys. Rev. B **52**, 17 099 (1995).

<sup>18</sup>M. V. Fischetti *et al.*, Phys. Rev. Lett. **55**, 2475 (1985).